MECHANICAL PERFORMANCE OF FIBRE REINFORCED CONCRETE: THE ROLE OF FIBRE DISTRIBUTION AND ORIENTATION

A. Abrishambaf [1], J.A.O. Barros[1], V.M.C.F. Cunha[1*],

[1] ISISE, Dep. Civil Eng., School Eng., University of Minho, Campus de Azurém 4800-058 Guimarães, Portugal.

ABSTRACT

Adding fibres to concrete provides several advantages, especially in terms of controlling the crack opening width after the cracking initiation of the composite. However, distribution and orientation of the fibres toward the crack plane are significantly important in order to provide the maximum benefit for controlling crack width. Therefore, in this study, the effect of the fibre distribution and orientation on the tensile behaviour of the steel fibre reinforced self-compacting concrete (SFRSCC) specimens is investigated. For this purpose, cores that are extracted from distinct locations of a panel will be subjected to indirect (splitting) and direct tensile tests. By modeling the splitting tensile test under the finite element framework and by performing an Inverse Analysis (IA), the achieved stress-crack opening relationship (σ-w) is compared with the one obtained directly from the experimental curve obtained in the direct tensile tests.

KEYWORDS: Fibre dispersion and orientation, Self-compacting concrete, Rheology, Tensile behaviour, splitting tensile test.

1. INTRODUCTION

Adding fibres to concrete provides several advantages, especially in terms of the controlling crack opening width, increasing the energy absorption capacity as well as the load bearing capacity of the structure when the composite is subjected to the tensile load [1-2]. Nevertheless, the contribution of the fibres becomes more effective after the crack initiation of the concrete. Crack opening in steel fibre reinforced concrete (SFRC) is counteracted by the bond stresses that develop at the fibres / matrix interface during the fibre pull-out. On the other hand, one of the most important properties of SFRC is its ability to transfer stresses across a cracked section rather uniformly, which nonetheless is dependent on the fibre reinforcement effectiveness, i.e. fibre properties (their strength, bond, and stiffness), and fibre orientation and distribution [3].

In order to optimize the maximum contribution of fibres for controlling crack width, it is important to evaluate the distribution and orientation of the fibres toward the crack plane. On the other hand, fibres are more effective fairly aligned mainly on the directions of the principal tensile stresses. The dispersion and orientation of fibres in the hardened-state results from a series of stages that SFRC passes from mixing to hardening state, namely [4]: fresh-state properties after mixing; casting conditions into the formwork; flowability properties; vibration and wall-effect introduced by the formwork. Among all the mentioned parameters, flowability of steel fibre reinforced self-compacting concrete (SFRSCC) is the most important one [5-7]. Having in the mind that, distribution/orientation of the fibres influences the mechanical properties of the SFRSCC significantly, it is important to control and consider both parameters, especially in terms of the design applications.

In this research the effect of the fibre distribution and orientation on the tensile behaviour of steel fibre reinforced self-compacting concrete (SFRSCC) is investigated. For this purpose, cores which are extracted from the various locations of a panel will be subjected to indirect (splitting) and direct tensile tests. By modeling splitting tensile test under the finite element framework and performing Inverse Analysis (IA), the numerical stress-crack opening relationship (σ-w) is compared with the obtained experimentally from the direct tensile test.

2. EXPERIMENTAL PROGRAM

2.1. Concrete mixture

A steel fibre reinforced self-compacting concrete was design with 60 kg/m^3 hooked end steel fibres (length, l_f, of 33 mm; diameter, d_f, of 0.55 mm; aspect ratio, l_f / d_f , of 60 and a yield stress of 1100 MPa). The material constituents are: cement (C), water (w), filler (F), fine sand (FS), coarse sand (CS), coarse aggregate (CA),

* Correspondent author. Tel.: +351 259 510 210
E-mail address: vcunha@civil.uminho.pt

superplasticizer (SP). Table 1 includes the concrete mix composition. In order to evaluate the flowability of the concrete, the slump test was performed based on the EFNARC recommendations [8]. The total spread achieved on the slump test was about 670 mm. To assess the properties of the concrete in the hardened state, Young's modulus and compressive tests were executed on the cylinders with a diameter of 150 and height of 300 mm. The average compressive strength (f_{cm}) and the average value of the Young's modulus (E_{cm}) were 47.77 MPa (7.45 %) and 34.15 GPa (0.21 %), respectively, where the values in parentheses represent the coefficient of variation.

Table 1- Mix composition of steel fibre reinforced self-compacting concrete per m^3.

C [kg]	W [kg]	SP [kg]	F [kg]	FS [kg]	CS [kg]	CA [kg]	Fibre [kg]
413	140	7.83	353	237	710	590	60

2.2. Specimens

Since casting panels from the centre improve mechanical behaviour comparing to other methods of casting, this method was selected for the production of two panels. The dimensions of the panels are 1600×1000×60 mm^3. In order to evaluate the influence of fibre dispersion and orientation on the tensile properties of SFRSCC, twenty-three cores were extracted from each panel to be tested in the indirect (splitting) and direct (uniaxial) tensile tests. The specimens were extracted along the concrete flow direct according to the scheme represented in Fig. 1. In this figure the pale dash lines with arrows represent the supposed concrete flow directions. The hatched cores were tested in the splitting tensile test and the others were kept for the uniaxial tensile test. For the execution of splitting tensile test, two notches were executed on the cores' opposite sides with the depth of 5 mm. In order to evaluate the influence of crack orientation towards the concrete flow, specimens were notched either parallel or perpendicular to flow direction. By assuming θ as the angle between the notched plane and the direction of the concrete flow, the notch plane was designated parallel for $\theta = 0^{\circ}$ or perpendicular for $\theta = 90^{\circ}$. Since the core scheme was maintained for both panels, for each core location there were two cores with distinct notch directions. This will enable to evaluate the influence of fibre orientation on the stress-crack width (σ-w) relationship. For instance, θ of A1 specimen is 90° and 0° in panels A and B, respectively.

The rest of the cores were sawn out to produce prismatic specimens with the dimension of 110×102×60 mm^3 to be used in uniaxial tensile test. Following the same notching procedure for the splitting test specimens, the prismatic specimens were notched according to parallel ($\theta = 0^{\circ}$) and perpendicular ($\theta = 90^{\circ}$) directions to the expected concrete flow. The notch was executed on the four lateral faces of the specimen, at theirs mid-height, with a thickness of 2 mm and a depth of 5 mm.

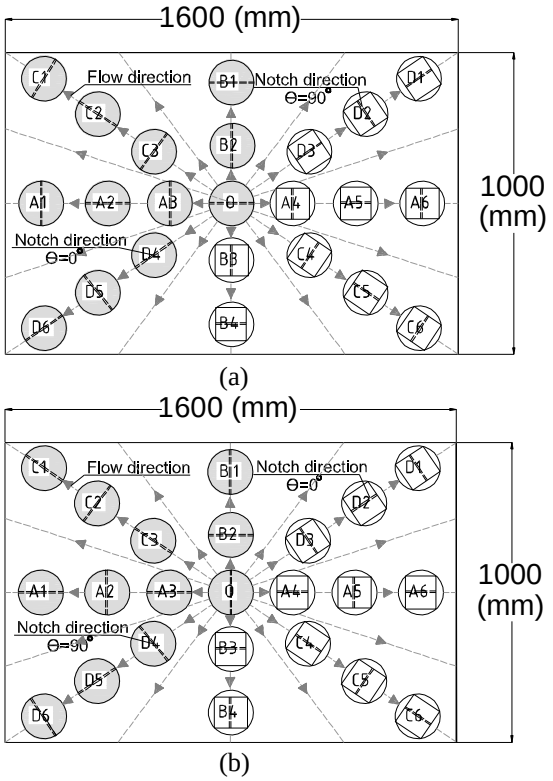

Figure 1. Core extracting plan: (a) panel A, (b) panel B.

2.3 Test setup

2.3.1 Splitting tensile test

In a first stage, the $\sigma - w$ relationship was assessed by executing splitting tensile tests following the recommendation of ASTM C-496 standard [9]. The tests were executed by closed-loop displacement control, using an external linear variable diferential transducer (LVDT) that was positioned on the actuator to control the vertical deformation of the specimen. To avoid a sudden drop in the value of the force, once the crack is initiated, a low value of displacement rate, i.e. 0.001 mm/s, was applied on the top of the notch. To record the crack opening width, five LVDTs were mounted of the surface of the specimen, three on the top and two on the bottom surface, see Fig. 2.

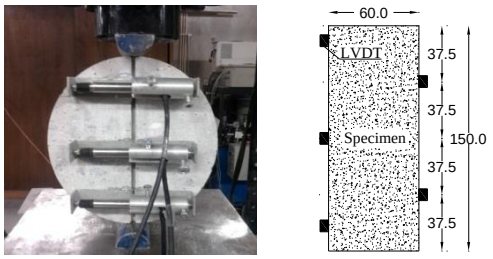

Figure 2. Geometry of the specimen and setup of the splitting tensile test (dimensions are in mm): (a) specimen front view (top of the panel), (b) specimen lateral view.

2.3.2 Uniaxial tensile test

To determine directly the stress – crack opening width ($\sigma - w$) relationship, uniaxial tensile tests were executed according to the RILEM TDF-162 [10]. This test was carried under closed-loop displacement control, adopting the following displacement rates during the test: 0.005 mm/min up to a displacement of 0.05 mm, 0.02 mm/min up to a displacement of 0.1 mm, 0.08 mm/min up to a displacement of 0.5 mm, and 0.1 mm/min until the completion of the test. The test was controlled by the averaging signal received from the four LVDTs installed on the lateral surface of each prismatic specimen, see Fig. 3.

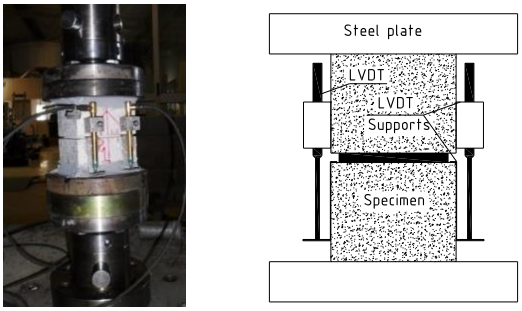

(a) (b)

Figure 3. Uniaxial tensile test setup: (a) specimen front view, (b) specimen lateral view.

2.4 Results and discussions

2.4.1 Splitting tensile test

Fig. 4 depicts the envelope and average force – crack mouth opening response ($F - w$) of the splitting tensile tests when the notch direction is parallel ($\theta = 0^{\circ}$) and perpendicular ($\theta = 90^{\circ}$) to concrete flow direction. During the first phase of the test, the F - w relationships were almost linear up to the stress at crack initiation. Until this displacement, the LVDTs recorded the elastic deformability of the SFRSCC between the supports; therefore this deformation should have been removed from the F - w curves. But since it was very negligible, the mentioned step had been ignored. After this stage, the composite exhibited non-linearity behaviour until the peak load was attained. Finally, this step was followed by a smoothly reduction in the residual forces, observing a softening phase.

In general, the $F - w$ relationship showed a high scattering. However, in the case of SFRSCC the scattering in the results is expected since the mechanical performance of this material depends on the fibre dispersion/orientation, even for the specimens from the same mixture and with the same testing conditions. In these results, because the specimens were extracted from different locations of the panels, i.e. with various distances from the casting point, the scattering in the results was expected. In fact, during the casting of the panels, the fibre distribution /orientation was influenced by viscosity of fresh matrix along the flowing process.

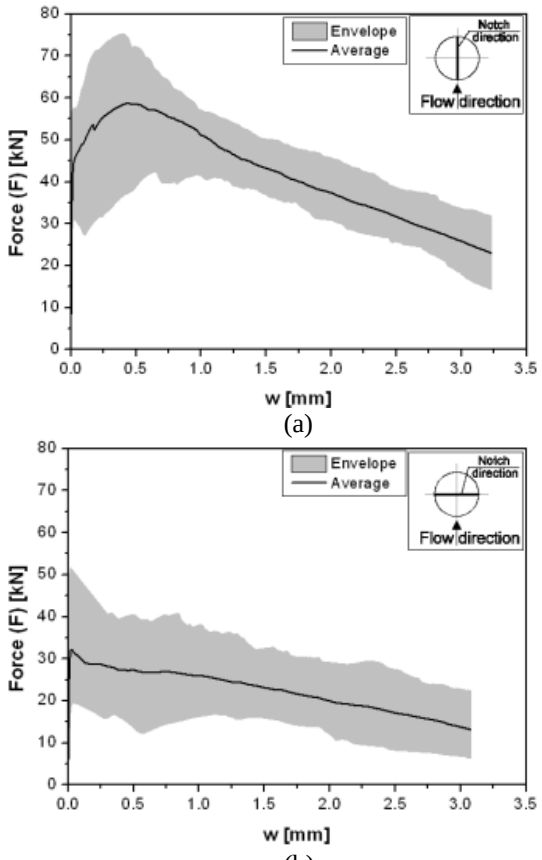

Figure 4. Force – crack opening width relationship, $F - w$, obtained from splitting tensile test for: (a) θ=0˚ and (b) $\theta = 90^{\circ}$.

2.4.2 Uniaxial tensile test

Fig. 5 illustrates the average and envelope force-crack mouth opening relationship for each series. The value of the crack opening was determined by averaging signals which were recorded in the four LVDTs. Similar to the previous section, for both series ($\theta = 0^{\circ}$ and 90°), the F - w curve is almost linear up to the load at crack initiation. This stage corresponds to the tensile strength of concrete. Once the tensile strength is attained, the force suddenly decreases up to a crack width about 0.07 mm. Beyond this crack width, $\theta = 0^{\circ}$ and 90° series show a completely different behaviour. A semi-hardening and a plateau responses are observed for the $\theta = 0^{\circ}$ and 90°series, respectively. Regarding the $\theta = 0^{\circ}$ series, Cunha *et al.* [11] have analyzed the micro-mechanical behaviour of hooked end fibres by performing fibre pull-out tests, and have verified that after a fibre sliding of nearby 0.1 mm, the fibre reinforcement mechanism is mainly governed by the hook plastification during the fibre pull-out process. Therefore, in this series, fibres start to be pulled-out slowly being observed a semi-hardening response. After this step, in $\theta = 0^{\circ}$ series, a plateau response was observed until the crack width of about 0.6 mm, then it

was followed by a smooth reduction in the residual forces. However, according to available experimental and analytical analysis, in order that active fibres bridging a leading crack become more efective, they should have an average orientation angle value lower or equal to 35°. Based on the fibre pull-out tests performed by Cunha et al. [12], fibre rupturing was the most predominant failure mode between the slip intervals of 0.6-1.0 mm, for the fibre inclination angle with the loading direction of 30°. Actually, during testing of the specimens under the tensile uniaxial load, once the peak load was achieved the sound of the fibre rupturing was clearly heard, which caused a rapid reduction in the value of the residual force. This was also confirmed by inspecting the fracture surface visually after the specimen testing.

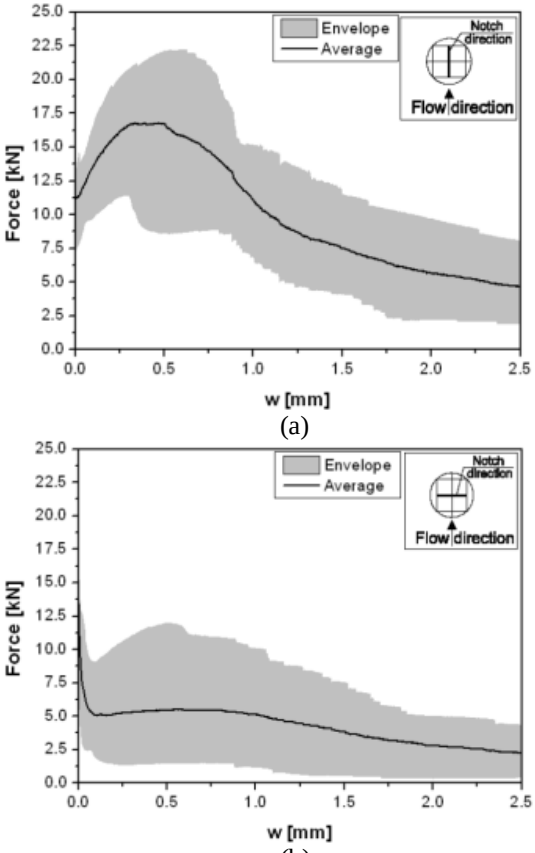

Figure 5. Force – average crack width relationship, *F - w*, obtained from the uniaxial tensile tests: (a) $\theta = 0^{\circ}$ and (b) $\theta = 90^{\circ}$.

In the case of $\theta = 90^{\circ}$, some specimens especially those located close to the centre of the panel (casting point) shown a pseudo-hardening behaviour. After this behaviour, a small plateau followed by a reduction of the residual force beyond a crack width of about 0.9 mm was observed, which corresponded to the rupture of the fibres.

Before the tensile strength of the material was attained (pre-peak branch), a low scattering of the results observed. The scattering increased after the tensile strength of the material was obtained and the crack initiated. In this step, the stress transferring across the surfaces of crack was transmitted from the matrix to the fibres, so the role of the fibres becomes more dominant. This process depends on how the fibres are distributed and oriented through the fracture surface which means the scattering observed in the post-peak branch is highly affected by the variation of these two parameters from one specimen to another one.

By comparing the results of the two series ($\theta = 0^{\circ}$ and 90°) in Figs. 5a and 5b, it is clearly noticeable that the influence of the notch orientation towards the concrete's flow on the post-peak behaviour of the material is quite high. The series with a notch inclination of $\theta = 0^{\circ}$ depicted a higher residual forces and hence dissipated a larger energy than the specimens with $\theta = 90^{\circ}$. The observed variation in the post-cracking parameters could be ascribed to a preferential fibre orientation at the crack surface. On the other hand, in the casting process of the panels from the centre, since the wall effects are negligible, the flow velocity is uniform and diffuses outwards radially from the casting point, see Fig. 6. Therefore, the fibres have a tendency to reorient perpendicular to the concrete flow direction. Consequently, in the $\theta = 0°$ series because of the high number of effective fibres with favourable orientation, the composite showed a semi-hardening response while in the $\theta = 90°$ series, since fibres were rotated due to the concrete flow velocity, the number of the effective fibres was reduced and lower residual forces were achieved.

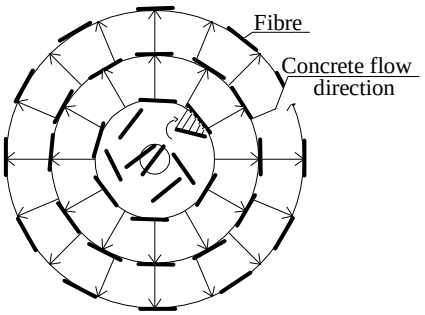

Figure 6. Explanation for fibre alignment in flowing concrete of a panel casting from the centre.

3. NUMERICAL SIMULATION

Generally, deriving mode I fracture parameters of the composites by executing uniaxial tensile test involves some difficulties such as the necessity of specialized and expensive equipment, sophisticated test set-up to avoid detrimental interferences, like load eccentricity, since it decreases the stress at the onset of crack initiation [13], therefore, this test is not so prevalent. Splitting tensile test could be considered as a more suitable option for this purpose because it is cheaper, less sophisticated testing equipment is needed, and can be executed on both cubes and extracted cores.

In this section a methodology to predict the stress – crack width ($\sigma - w$) relationship of SFRSCC of laminar structures using an inverse analysis, IA, procedure on the results of the splitting tensile test will be discussed. For this purpose, numerical simulations of the splitting tensile results with a nonlinear 3D finite element model were performed. In order to confirm the accuracy of the proposed methodology, the $\sigma - w$ response obtained indirectly was compared to the one obtained from the uniaxial tensile test, which renders the direct $\sigma - w$ relationship.

3.1 Modelling and simulation

The experimental force – crack width responses of the splitting tensile tests (Fig. 4) were simulated using ABAQUS® finite element software [14]. By using an appropriate element and material model available in the ABAQUS® program library [15, 16], the geometry of the specimen and material properties were simulated. Because of the symmetry in the specimen geometry, supports and test loading applied in the splitting tensile test, only a quarter of the core was simulated, see Fig, 7a. Since the specimen had distinct thicknesses in the notch and un-notch part, the geometry of the specimen consists of two main parts namely: Notch and Un-notch (flush). After meshing each part individually, the assembled mesh is shown in Fig. 7b with a total number of 5674 elements. The type of the elements was 8-node hexahedral shape solid element with 8-integration points. Similar to the experiment, in the numerical simulation a non-zero prescribed displacement was applied on top of the notch to model the softening phase of the material with enough accuracy.

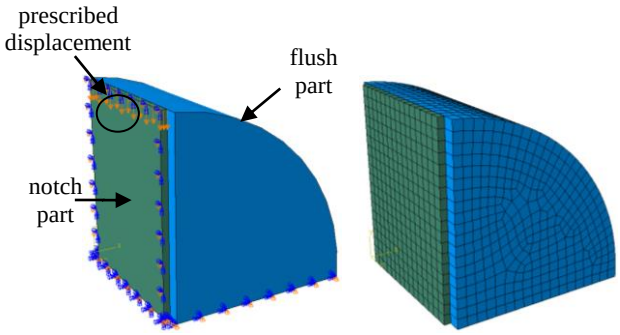

Figure 7. Three-dimensional view of numerical model: (a) Geometry, constraints and prescribed displacement, (b) Finite element mesh.

3.2 Concrete constitutive model

The concrete damage plasticity, CDP, model was used to model the mechanical performance of concrete because it is proficient to simulate the cracking of concrete in tensile and crushing in compression. On the other hand, this model uses the concept of isotropic damage elasticity in combination with isotropic compression and tension plasticity to simulate the inelastic behaviour of concrete under compressive and tensile stresses. Table 2 depicts the implemented initial parameters of CDP model to simulate the concrete response during execution of splitting tensile test.

Table 2. The constitutive parameters of CDP model.

Dilatation angle [degrees]	40
Eccentricity, e [-]	0.1
σ_{bo}/σ_{co} [-]	1.16
K_c [-]	0.667

In this model, when the compressive strength is attained, the concrete shifts to the softening phase. On the other hand the compressive inelastic strain used is defined by subtracting the elastic strain component from the total strain of the relationship derived in the uniaxial compressive test. Table 3 contains the mechanical properties parameters used on numerical simulation.

Similar to the compressive response, the model shows a linear tensile behaviour until the stress reaches the tensile strength of concrete which coincide with cracking of the material. Afterward, the stress follows a descending behaviour representative of the softening phase. The SFRC softening phase is expressed as a function of cracking strain which can be determined by subtracting the elastic strain corresponding to the undamaged part from the total strain.

Table 3. Mechanical properties adopted in the numerical simulations.

Density, ρ	2.4×10^{6} N/mm^3
Poisson ratio, υ	0.2
Initial young modulus, E_{ci}	34.15 N/mm^2
Compressive strength, f_{cm}	47.77 N/mm^2
Tensile strength	Inverse analysis
Post-cracking parameters	Inverse analysis

3.3 Inverse analysis procedure

By fitting the numerical load – crack width curve to the correspondent experimental average curve, the values σ_i and w_i that define the tensile stress – crack width law were computed. The procedure consists of three main stages: Firstly, a preliminary estimation of the uniaxial tensile behaviour was set in to the program and a limit for error in the numerical simulation was also assumed $err_f = 5\%$. Secondly, from the nonlinear finite element analysis, the numerical load – crack width response, $F_{NUM} - w$, was determined. Finally, the obtained numerical $F_{NUM} - w$ relationship was compared to the experimental one, $F_{EXP} - w$, and the normalized error, err, was computed as follows:

$$err = \sum_{i=0}^{w_u} \left| F_{iEXP} - F_{iNUM} \right| \Big/ \sum_{i=0}^{w_u} F_{iEXP} \qquad (1)$$

where F_{iEXP} and F_{iNUM} were the experimental and the numerical load value at i^{th} crack width value, respectively. The final $\sigma - w$ relationship was defined by the parameters set that lead to the lowest normalised error between the experimental and numerical compressive force versus crack width curves.

3.4 Numerical results, validation and discussion

Fig. 8 illustrates a comparison between the average and envelope ($EXP_{SPLT}Avg$ and $EXP_{SPLT}Envelope$ respectively) experimental force – crack width curves achieved by the execution of splitting tensile test and the numerical response obtained from inverse analysis (NUM_{SPLT}). The numerical analysis was performed up to the crack width of 2 mm in the centre of the specimen. As represented in Fig. 8, a good accuracy between the experimental and numerical simulation was achieved, even though a slight difference was observed, but the estimated error (*err*) was lower than 5 %.

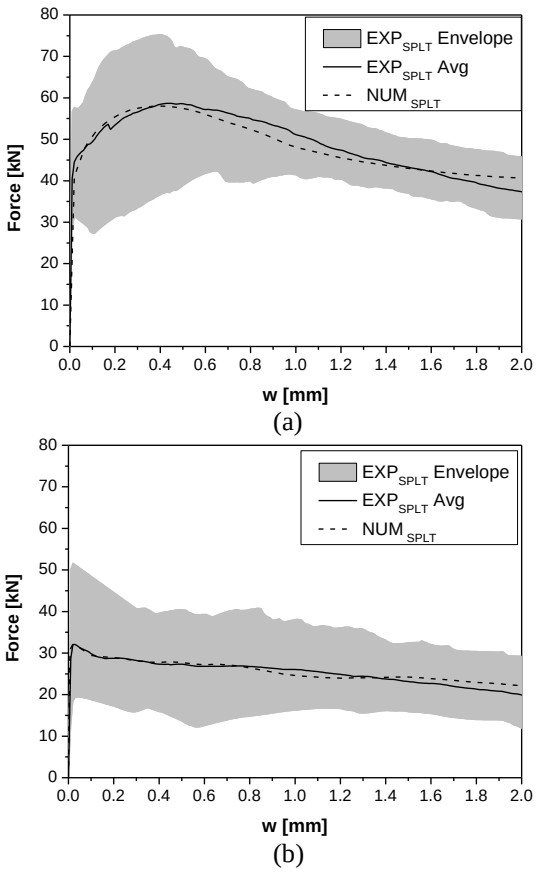

Figure 8. Experimental and numerical force – crack width relationship, *F-w*, for: (a) $\theta = 0^{\circ}$ and (b) $\theta = 90^{\circ}$.

Fig. 9 depicts the $\sigma - w$ relationship from the inverse analysis that lead to the smallest error, based on the methodology previously explained. The numerical tensile strengths were determined as 3.6 and 3.2 MPa for $\theta = 0^0$ and $\theta = 90^0$ specimens, respectively. By comparing the response for both series, similar to the uniaxial tensile test, the post-cracking residual stresses in $\theta = 0^0$ series was significantly higher due to the fibre tendency to be reoriented perpendicular to concrete flow direction in the case of casting panels from the centre. Therefore, in $\theta = 0^0$ specimens there are more effective fibres to bridge the crack plane than $\theta = 90^0$ series.

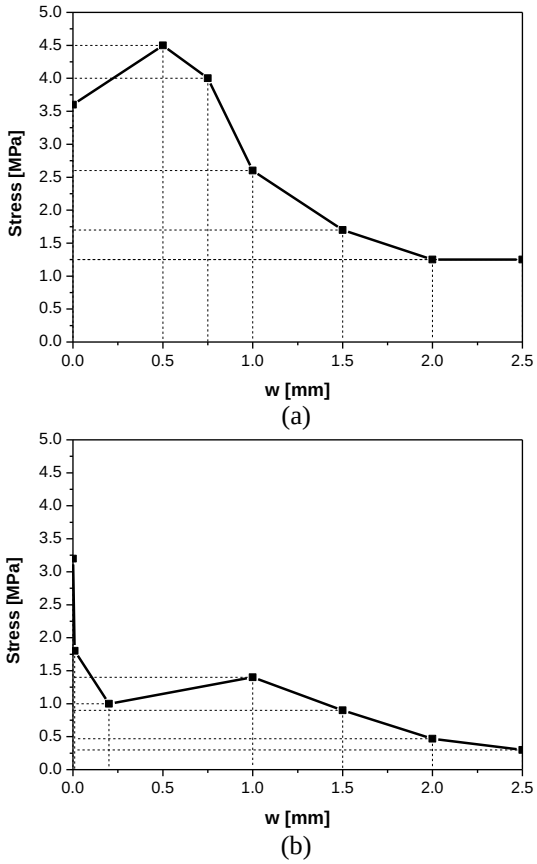

Figure 9. Numerical uniaxial stress – crack width relationship, $\sigma - w$, obtained from inverse analysis for: (a) $\theta = 0^{\circ}$ and (b) $\theta = 90^{\circ}$.

3.5 Comparison of results

Figs 10 and 11 shows for each series the uniaxial $\sigma - w$ relationships obtained from the inverse analysis procedure of the splitting tensile test (NUM_{SPLT}), the envelope and average curves from uniaxial tensile test ($EXP_{UTT}Envelope$, $EXP_{UTT}Avg.$) carried out according to the RILEM TDF-162 recommendations [2]. Moreover, the $\sigma - w$ response for the splitting test was determined from Eq. 2 as proposed by ASTM C-496 standard (EXP_{SPLT}) [9] is also represented.

$$\sigma_{SPLT} = \frac{2F}{\pi l d} \tag{2}$$

Where F is the applied line load, d is the diameter of the cylinder (150 mm) and l is the thickness of the net area in the notched plane (50 mm).

The $\sigma - w$ relationship achieved by the inverse analysis procedure rendered a relatively good approximation of the uniaxial tensile response, principally, for the series $\theta = 90^{\circ}$. NUM_{SPLT} and EXP_{SPLT} approaches showed a very

close tensile strength, which were higher than EXP_{UTT} Avg. However, according to the literature, splitting tensile test slightly overestimated the tensile strength compared to the uniaxial tensile test. At the early cracking stages (w < 0.6 mm) NUM_{SPLT} and EXP_{SPLT} methods rendered $\sigma - w$ response nearby upper bound limit of the EXP_{UTT} Envelope, this overestimation could be ascribed to the effects of the compressive stress along the loading plane.

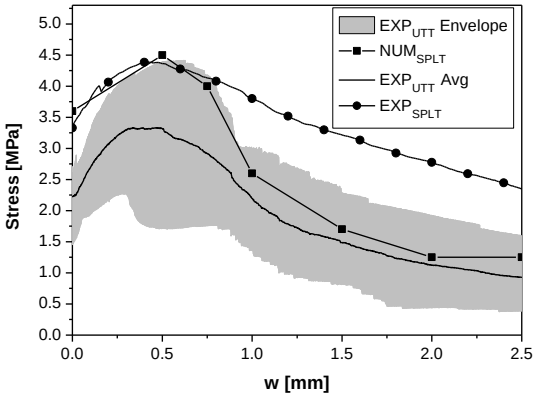

Figure 10. Comparison of the uniaxial stress – crack width relationship, $\sigma - w$, for $\theta = 0^{\circ}$.

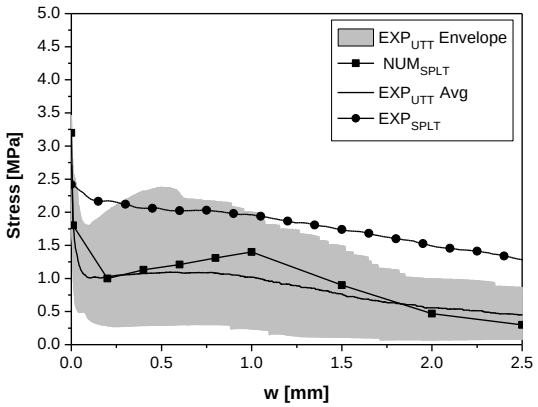

Figure 11. Comparison of the stress – crack width relationship, $\sigma - w$, for $\theta = 90^{\circ}$.

Once the crack gets wider, since in EXP_{SPLT} method, stress was determined from Eq. 2 that assumes a linear elastic stress distribution even after cracking of the matrix, this method was unable to predict post-cracking tensile response with enough accuracy. But, NUM_{SPLT} started to get closer to the response obtained from the uniaxial tensile test.

Regarding the tensile strength in $\theta = 90^{\circ}$ series (see Fig. 11), like the previous series, inverse analysis procedure of the splitting tensile tests overestimated it when comparing to the tensile strength obtained from the uniaxial tests, although it was within the experimental envelope. According to the EXP_{UTT} results, a sharp stress reduction happened once the crack initiated due to the brittle nature of the matrix and existing lower number of effective fibres in the fracture plane. The sudden decay of the stress was stopped when the hook of the fibres started to deform, which happened at a crack width between [0.1 – 0.3] mm depending on the length of the fibre's hook. The result of the inverse analysis method reproduced the EXP_{UTT} response with a good accuracy since in this series a majority of the elements were subjected to tensile stress in horizontal as well as vertical directions. Unlike previous series (θ= 0°) that showed a signifficant high residual stresses, this series had a much lower post-cracking residual stresses, therefore the load bearing capacity of the specimen has decreased and the compressive stresses were not so preponderant in the overall response.

4. CONCLUSION

In this study, the influence of fibre dispersion /orientation of the tensile post-cracking parameters of steel fibre reinforced self-compacting concrete panel was investigated. The $\sigma - w$ law was determined indirectly by performing inverse analysis on the experimental results of splitting tensile test as well as directly by executing uniaxial tensile test. According to experimental and numerical investigations, the following conclusions could be derived out:

The tensile behaviour of the drilled specimens from the panel was influenced by the fibre dispersion and orientation significantly. Specimens with notch direction parallel to concrete flow ($\theta = 0^{\circ}$) represent a much higher post-cracking residual stresses than the other investigated case when the notch direction was perpendicular to the flow direction ($\theta = 90^{\circ}$).

In the case of casting panels from the centre, fibres have a tendency to align perpendicular to the radial flow, mainly due to the uniform flow profile velocity that diffuses outwards radially from the centre of the panel. Consequently, the total number of the effective fibres was higher in parallel crack plane ($\theta = 0^{\circ}$) in order to transfer stress across the crack surface comparing to the other case registered in the orthogonal crack plane ($\theta = 90^{\circ}$).

The inverse analysis of the splitting tensile response can anticipate with a relatively good accuracy the uniaxial tensile behavior, in particular, for low fibre contents. Although the proposed methodology tends to slightly overestimate the response achieved from the uniaxial tensile test in the case of high content of fibres ($\theta = 0^{\circ}$), but this response could be dilute by the scattering of SFRSCC material which exist due to the fibre dispersion and orientation.

ACKNOWLEDGEMENTS

This work is supported by the FEDER funds through the Operational Program for Competitiveness Factors - COMPETE and National Funds through FCT - Portuguese Foundation for Science and Technology under the project SlabSys - HFRC PTDC/ECM/120394 /2010. The authors would like to acknowledge the

materials supplied by Radmix and Maccaferri (fibres), SECIL (cement), SIKA and BASF (superplasticizers), Omya Comital (limestone filler), and Pegop (Fly ash).

REFERENCES

[1] ACI 544–1R, 2002, "State-of-the-art report on fiber reinforced concrete", Technical report, American Concrete Institute, 2002.

[2] P.N., Balaguru, S.P., Shah, 1992, "Fiber reinforced cement composites", McGraw-Hill Inc., New York.

[3] L., Vandewalle, D., Dupont, 2003, "Bending test and interpretation, test and design methods for steel fibre reinforced concrete", background and Experiences, RILEM publication PRO 31, Bagneux, 1-14.

[4] F., Laranjeira, 2010, "Design-oriented constitutive model for steel fiber reinforced concrete", PhD thesis, Universitat Politècnica de Catalunya.

[5] L., Ferrara, A., Meda, 2006, "Relationships between fibre distribution, workability and the mechanical properties of SFRC applied to precast roof elements", Materials and Structures, vol. 39, pp. 411-420.

[6] W., Pansuk, H., Sato, Y., Sato, R., Shionaga, 2008, "Tensile behaviours and fibre orientation of UHPC", *In Proceedings of Second International Symposium on Ultra High Performance Concrete*, Kassel, Germany (Kassel University Press), pp. 161-168.

[7] S.W., Kim, S.T., Kang, J.J., Park, G.S., Ryu, 2008, "Effect of filling method on fibre orientation and dispersion and mechanical properties of UHPC", *Proceedings of Second International Symposium on Ultra High Performance Concrete*, Kassel, Germany (Kassel University Press), pp. 185-192.

[8] EFNARC, 2005, "The European guidelines for self-compacting concrete".

[9] ASTM C496, 2004, "Standard test method for splitting tensile strength of cylindrical concrete specimens", Annual Book of ASTM Standards, American Society of Testing Materials.

[10] RILEM TC162-TDF, 2001, "Test and design methods for steel fibre reinforced concrete: Uniaxial tension test for steel fibre reinforced concrete", Materials and Structures, vol.34, pp. 3-6.

[11] V.M.C.F., Cunha, J.A.O., Barros, J.M., Sena-Cruz, 2010, "Pullout behaviour of Steel Fibres in Self Compacting Concrete", ASCE Journal of Materials in Civil Construction, vol.22, pp. 1-9.

[12] V.M.C.F., Cunha, J.A.O., Barros, J.M., Sena-Cruz, 2011, "An integral approach for modeling the tensile behaviour of steel fibre reinforced self-compacting concrete", Cement and Concrete Research, vol.41, pp. 64-76.

[13] F.P., Zhou, 1988, "Some aspects of tensile fracture behaviour and structural response of cementicious materials". Report no. tvbm-1008, division of building materials, Lund Institute of Technology, Lund, Sweden.

[14] Abaqus Unified FEA software, 2009, "User Manual", Dassault Systèmes Simulia Corp., Providence, RI, USA.

[15] Abaqus Unified FEA software, 2009, "Analysis user's manual, Volume IV: Elements", Dassault Systèmes Simulia Corp., Providence, RI, USA.

[16] Abaqus Unified FEA software, 2009, "Analysis user's manual, Volume III: Materials". Dassault Systèmes Simulia Corp., Providence, RI, USA.